Journal of Drug Delivery Science and Technology 87 (2023) 104804

Contents lists available at ScienceDirect

Journal of Drug Delivery Science and Technology

journal homepage: www.elsevier.com/locate/jddst

Supercritical millifluidic process for siRNA encapsulation in nanoliposomes for potential Progeria treatment (*ex-vivo* assays)

Mathieu Martino [a,*], Adil Mouahid [a], Michelle Sergent [b], Camille Desgrouas [c,d], Catherine Badens [c,d,e], Elisabeth Badens [a]

[a] Aix Marseille Univ, CNRS, Centrale Marseille, M2P2, Marseille, 13451, France
[b] Aix Marseille Univ, IMBE, UMR CNRS IRD Avignon Université, Site de l'Etoile, Marseille, France
[c] Aix Marseille Univ, INSERM, MMG, Marseille, France
[d] Aix Marseille Univ, Laboratoire de Chimie Analytique, Faculté de Pharmacie, Marseille, France
[e] APHM, Hôpital de la Timone, Laboratoire de Génétique Moléculaire, 13005, Marseille, France

ARTICLE INFO

Keywords:
Nanoliposomes
Supercritical fluids
Process optimization
Millifluidic process
siRNA encapsulation
Progeria

ABSTRACT

A millifluidic process working in continuous mode for the preparation of nanoliposomes using supercritical CO_2 has been developed. Nanoliposomes with an average diameter ranging between 123.9 ± 3.0 and 165.7 ± 1.6 nm depending on the operating conditions were obtained. The effects of pressure (90–150 bar), temperature (35–45 °C) and phospholipid mass ratio (0.1–1.9 wt%) in feed solution on liposome sizes were investigated. The concentration of phospholipids was found to be the most significant parameter for controlling the mean diameter of nanoliposomes while pressure and temperature had a minor influence on liposomes' properties. The encapsulation of siRNAs targeting the *LMNA* gene by nanoliposomes obtained with the millifluidic process was achieved at optimized operating conditions (150 bar, 35 °C and a phospholipid mass ratio in the feed solution of 0.1 wt%). The resulting formulations were compared with commercial transfection agents in *ex vivo* assays. These assays showed a decrease in the expression of the encoded protein lamin A for the formulations obtained with the process developed in this work. Therefore, the use of siRNAs targeting *LMNA*, encapsulated by nanoliposomes represents a potential new therapeutic approach for the treatment of progeria.

1. Introduction

Since the late 1990s, small new non-coding RNAs have been described which are involved in the regulation of gene expression through a mechanism called RNA interference (RNAi) [1,2]. The small-interfering RNAs (siRNAs) represent an alternative to conventional drug therapies targeting disease-related proteins [3,4] as they can specifically inhibit the expression of a gene. Indeed, siRNAs make it possible to modulate the expression of genes by degrading messenger RNAs (encoding the genetic information for the synthesis of proteins in cells), or by inhibiting their translation into proteins. These interfering RNAs are used in particular in cancerology or virology in order to reduce the expression of a specific gene or to inhibit the increase in viral loads [5,6]. The advantage of this type of therapy is linked to specific RNAs targeting, something that allows treatments with fewer side effects [7]. However, siRNAs are very unstable in the organism [8]. They are quickly degraded *in vivo* by the action of ribonucleases and are sensitive to pH variations in the organism [9,10].

A possible way to protect nucleic acids following their administration is the use of liposomes, which are soft matter vesicular carriers, non-toxic and biodegradable that can protect RNAs and enhance their delivery [11–15]. The phospholipidic bilayers that mimic cell membranes make liposomes the first choice for encapsulating matrices in therapy [16,17]. The main limitation for the use of liposomes as drug carriers for gene or cancer therapy is their size. Indeed, the particle size is a key characteristic for the particle cellular internalization. Particle with a size up to 5 μm can undergo a cell internalization, but the process is more rapid for particles with a size smaller than 150 nm [18,19]. It is commonly accepted that the recommended particle diameter for treating cancer is in the range of 10–150 nm, and nanoparticles in the range of 10 nm penetrate cells more effectively, using pathways of cell internalization which limit degradation.

Conventional methods of liposome preparation have been developed for several decades (Bangham method, reverse phase evaporation, solvent injection, detergent) [20–25]. However, these simple techniques

* Corresponding author.
E-mail address: mathieu.martino@univ-amu.fr (M. Martino).

https://doi.org/10.1016/j.jddst.2023.104804
Received 20 February 2023; Received in revised form 10 July 2023; Accepted 31 July 2023
Available online 8 August 2023

Abbreviationlist

DDS	Drug Delivery System
DLS	Dynamic Light Scattering
MD	Mean Diameter
PDI	PolyDispersity Index
SD	Standard Deviationv
RNA	Ribonucleic Acid
RSM	Response Surface Methodology
siRNA	Small interfering Ribonucleic Acid
HGPS	Hutchinson-Gilford Progeria Syndrome
WB	Western Blot

require the use of toxic organic solvents. Furthermore, these methods do not allow a good control of the liposome properties (size, size distribution, encapsulation efficiency) [21]. Consequently, the liposomal suspensions formed are relatively unstable. These classical methods are not the most suitable for the preparation of nanoliposomes for siRNA encapsulation.

In order to overcome the problems associated with conventional methods, several techniques for liposome formation using supercritical fluids have been developed. Methods based on supercritical fluid, especially supercritical CO_2 ($scCO_2$) [26], allow the control of the final characteristics of the liposomes forming small vesicles [27–32] with good repeatability. $ScCO_2$ is an interesting alternative to organic solvents as CO_2 is nontoxic, non-flammable and its use has led to the reduction of the quantity of required organic solvent for drug production and formulation. At industrial scale, CO_2 is recycled, enabling a green and compact process with limited or even zero discharges and emissions. Several supercritical processes have been developed with a distinction made based on whether the supercritical fluid is used as a solvent or as an antisolvent for the phospholipids [33]. These processes can operate continuously or in batch mode. Depending on the processes used, the size of the liposomes formed can range from 10 nm to 1000 μm and they can have different lamellarities (unilamellar or multilamellar). Among these methods, the most commonly used processes are: Supercritical Reverse Phase Evaporation (scRPE), Depressurization of an Expanded Solution into a Aqueous Media (DESAM), Supercritical Assisted Liposome Formation (SuperLip), Supercritical AntiSolvent (SAS) [26]. The advantages and limitations of these different processes are discussed in the literature [26]. The choice of process is essentially based on the desired characteristics of the liposomes formed.

The objective of this work was to develop a $scCO_2$ millifluidic process operating in a continuous mode for the preparation of nanoliposomes with a diameter of less than 150 nm in order to encapsulate siRNAs and to evaluate the efficacy of the formulations to modulate gene expression, following a specific model that could be used as a therapeutical approach. Hutchinson-Gilford progeria syndrome (HGPS) is a rare genetic disease causing premature ageing, growth retardation and heart disease [34] and represents an excellent model of potential gene targeted therapy. The molecular cause of the disease is a mutation of the *LMNA* gene leading to the production of an abnormal protein lamin A called progerin which is toxic and leads to an alteration of the nuclear envelope structure and function [35]. The use of siRNAs to decrease *LMNA* expression is known to reduce the progerin level and nuclei alterations and thus constitutes a potential therapeutic strategy [36]. As the effect of *LMNA*-targeted siRNA can be followed in cell culture by the relative quantification of lamin A after treatment, it is a convenient model to evaluate siRNA encapsulation efficacy and safety [35]. The encapsulation of this siRNA model will allow the study of both the efficiency of the process implemented and the efficiency of the formulations obtained for the treatment of HGPS.

The development of this millifluidic process is part of a process intensification approach consisting of reducing the size of the installations and in having a more flexible use of the process. Using millimetric tubings as a millifluidic device in place of large high-pressure vessels reduces the investment and operating costs. The production capacity can easily be increased by numbering-up the millifluidic devices. Some scale-up issues such as the change of the formed vesicle size linked to the change of vessel or tubing size can thus be totally avoided. The preparation of liposomes using millifluidic devices with supercritical CO_2 has been implemented and described in the work of Murakami et al. [37]. The process described in this latter work for the preparation of liposomes consists of a specific micromixer and a four-pump injection system for introducing the different phases required to form liposomes. The process presented in this work allows the preparation of liposomes in classical commercially available stainless steel tubings and by reducing the size of the compound injection device. In fact, the compounds needed to form liposomes (water and phospholipids) are injected in a single phase constituting the single feed solution of the process. The process therefore requires a single pump to inject the compounds used to prepare the liposome and a second pump to supply the device with CO_2 reducing the total amount of pump required. The resulting process is therefore compact, with reduced CAPEX and OPEX costs.

The first step of this work was to study the influence of the variation of operating conditions (pressure: 90–150 bar, temperature: 35–45 °C and phospholipid mass ratio: 0.1–1.9 wt%) upon the liposome average diameter (without nucleic acids) using response surface methodology (RSM). RSM is a useful tool allowing the selection of the optimal operating conditions for the formation of nanoliposomes with an adequate size for the targeted application, this being the encapsulation of siRNAs.

The second step consisted of the experimental study of the siRNA's encapsulation at the previously selected operating conditions. *Ex vivo* transfection assays were performed to evaluate the efficacy of the formulations in comparison with commercial training kits for the decrease of the expression of lamin A.

2. Materials and methods

2.1. Materials

The source of phospholipids used is L-α-phosphatidylcholine from egg yolk (100% purity, Sigma-Aldrich, Saint-Quentin, France). The phospholipids were solubilized in absolute ethanol (99.8%, VWR, Rosny-sous-Bois, France), and in distilled water directly produced in our laboratories. Carbon dioxide (>99.7% purity, Air Liquide France) was used in the millifluidic process. The two types of encapsulated RNA were synthesized by the company Eurogentec (Seraing, Belgium) and provided in a lyophilized form. The first one is a *LMNA*-antisense siRNA duplex that specifically targets the *LMNA* transcript (3′UTR region) with the following sequences:

- UUU-UCU-AAG-AGA-AGU-UAU-U99
- AAU-AAC-UUC-UCU-UAG-AAA-A99

The second one is a siRNA universal negative control with a confidential sequence that does not target any gene (SR-CL005-005, Eurogentec, Fremont, CA, USA). The antisense sequence is a sequence able to bind to the *LMNA* gene and thus modulate the expression of the corresponding protein lamin A/C, which constitutes a potential therapy for the treatment of Hutchinson-Gilford Progeria Syndrome (HGPS) in this study.

2.2. Feed solution preparation

The feed solution containing the phospholipids was prepared in a water/ethanol solution (79/21% w/w) at room temperature (20 °C). The proportion of water/ethanol has been optimized in previous works [31,38]. In a first step, L-α-phosphatidylcholine (0.3, 2.9 or 5.5 g

depending on the desired lecithin mass ratio, respectively 0.1, 1.0 and 1.9 wt%) was dissolved in ethanol (61.5 g). The solution was stirred with a magnetic stirrer until the phospholipids were totally dissolved, then distilled water (228.5g) was added to the solution and stirred again. According to the phosphatidylcholine-ethanol-water phase diagram presented in the work of Söderberg [39], the process feed solution is characterized by the presence of two phases: a liquid phase and a lamellar phase across the entire phospholipid concentration range studied. The feed solutions for RNAs encapsulation were prepared using a phospholipid mass ratio of 0.1 wt%. The RNAs were added to the feed solution to reach a concentration of RNA (*LMNA*-antisense and negative control) of 5 μM.

2.3. Experimental set-up

The continuous millifluidic process experimental set-up is shown in Fig. 1. The stainless-steel high pressure millifluidic device (AM) is composed of a 1/4" tube (Top Industrie, France) with an internal volume of 1.2 mL (internal diameter of 3.87 mm, length of 10 cm and length/diameter ratio of 2.58). This volume reduction allows the formulation of liposomal suspensions in smaller quantities (useful for the encapsulation of costly molecules). It was equipped with a double jacket connected to a heating bath circulator (E2) to ensure a homogeneous working temperature in the whole autoclave. Internal temperature was measured with a type K thermocouple (TI) inserted into a thermowell.

CO_2 was primarily cooled thanks to a cold bath circulator (E1) at 0 °C to ensure the CO_2 liquid state before being introduced into the pump. A liquid high-pressure pump (P1 - HPP6/LGP50, Separex, Champigneulles, France) was used to pressurize CO_2 up to the working pressure (90, 120 or 150 bar). High pressure CO_2 was preheated to the desired temperature (E2) and then injected into a 0.48 L buffer autoclave (AT – Top Industrie, Vaux-le-Pénil, France) equipped with a water jacket connected to E2 to ensure constant temperature. The buffer autoclave allows the supply of $scCO_2$ into the working millifluidic device (AM) without a sudden change in pressure when the micrometering outlet valve (MV1) is open. A buffer tank is used at industrial scale and placed in the CO_2 recycling loop. Once sc CO_2 was introduced into the millifluidic device (AM) at the working pressure and stabilized at the working temperature (35, 40 or 45 °C), the micrometering valve (MV1-connected at its exit to a 1/16" stainless-steel high-pressure tube of 0.5 mm internal diameter) at the outlet of the process was opened to obtain a constant CO_2 flow rate of 8.65 g min^{-1}. This flow makes it possible to have a continuous process (the heated MV1 valve does not freeze during depressurization). This output flow rate was kept constant during the whole liposome formation protocol. To be able to continuously recover liposomal suspension, the micrometering valve is heated by a heating wire wound on the valve. This heating wire allows to evacuate the ice formed during the expansion of the mixture. This heating wire is left running for the duration of the test (90 min). The system was left to equilibrate for 10 min to ensure a constant temperature into the millifluidic device. After equilibrium time, the feed solution was injected through a high-pressure liquid pump (P2 Gilson 305, Villiers-le-Bel, France) at a flow rate of 1 mL min^{-1}. Before being introduced into the device, the pre-heated (E2) feed solution passed through a stainless-steel frit (S1 - 2 μm porosity) placed at the top of the millifluidic device. $ScCO_2$ and feed solution were injected into the millifluidic device through a T-connection. Upon depressurization of the continuously injected feed solution, the liposomal suspension was recovered in a hermetic Erlenmeyer flask cooled to 0 °C by placing it in a water and ice bath. During the production of nanoliposomes, the pressure into the millifluidic device (AM) was maintained constant by the automatic pressure regulation of P1. The CO_2 injection pump (P1) was equipped with a regulation system. The pressure inside the millifluidic device was regulated directly by the P1 pump by increasing or decreasing the CO_2 injection rate to maintain a constant pressure during the test period (90 min). When 90 mL of the feed solution was injected, pump P2 was stopped, and pure

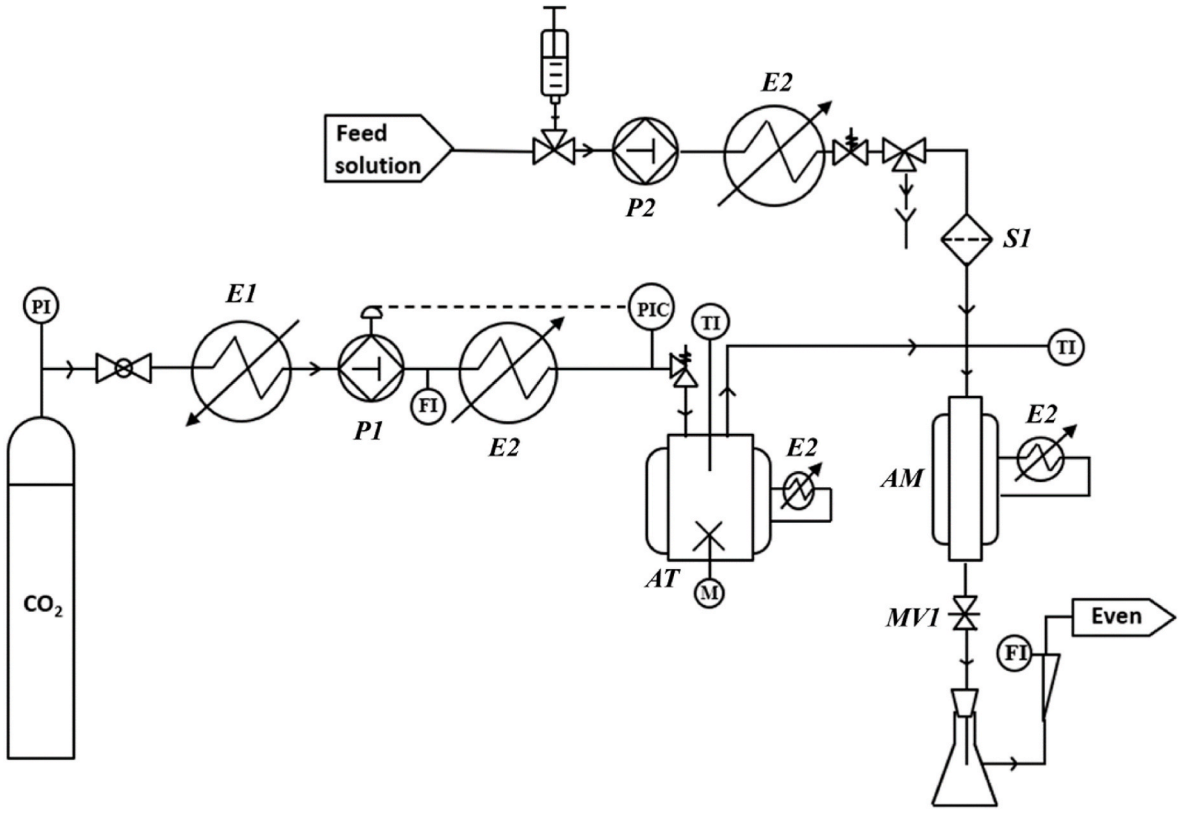

Fig. 1. Experimental set-up of continuous millifluidic process for nanoliposome preparation (AM: millifluidic device; AT: buffer autoclave; E1: cold bath circulator; E2: hot bath circulator; MV1: micrometering valve; P1 and P2: liquid high pressure pump; S1: stainless-steel frit).

$scCO_2$ was introduced into AM for 10 min (constant pressure and output flow). $ScCO_2$ injection was then stopped for complete depressurization. The liposomal suspension formed was recovered and passed through a rotary evaporator at a temperature of 30 °C (Laborota 4000, Heidolph, Germany) to evaporate ethanol without degradation of the liposomes formed.

A representation of the mechanism of liposome formation in supercritical process is shown in Fig. 2. The aqueous-organic solution containing the phospholipids is injected into the device. This device is previously charged with $scCO_2$. The injection of the feed solution into $scCO_2$ leads to the formation of a CO_2-in-water or water-in-CO_2 emulsion depending on operating conditions and on the global composition in the millifluidic device [40]. A new type of emulsion appears during depressurization. Indeed, the spontaneous CO_2 release during depressurization induces the formation of a water-in-water emulsion. This emulsion results from the specific organization of phospholipids in water, forming liposomes [40].

2.4. Liposome characterization

Size and size distribution of liposomal suspensions were characterized by a dynamic light scattering (DLS) instrument (Zetasizer nano S, UK) allowing the measurement of size in the range of 0.3 nm–10 000 nm. The mean diameter (MD) associated with Standard Deviation (SD) was characteristic of liposome size. The polydispersity index (PDI) with its associated standard deviation was characteristic of liposome size distribution. A He-Ne laser (4 mW, 633 nm) was used as the light source of the Zetasizer instrument. Each sample was measured 5 times at 25 °C in a 10 mm quartz glass cell (Hellma, Germany). An average result was taken for all experiments and the error bars were determined by calculating the standard deviation of all the measurements.

2.5. Experimental design and response surface methodology

The effects of pressure (90–150 bar), temperature (35–45 °C) and phospholipid mass ratio in the feed solution (0.1–1.9 wt%) on the mean diameter (MD) and PDI factor of the nanoliposomes formed was studied by RSM. Response Y (MD in nm and PDI factor) was modelled by a second-degree polynomial model given by Eq. (1).

$$Y = b_0 + b_1.P + b_2.T + b_3.C + b_{1-1}.P^2 + b_{2-2}.T^2 + b_{3-3}.C^2 + b_{1-2}.P.T + b_{1-3}.P.C + b_{2-3}.T.C \quad (1)$$

Where P is the pressure, T is the temperature, C is the phospholipid mass ratio expressed in unidimensional values and b_i are the modelling coefficients.

In order to determine the modelling coefficients of the model, a Box-Behnken design was used and a plan with 13 experiments (Table 1) with

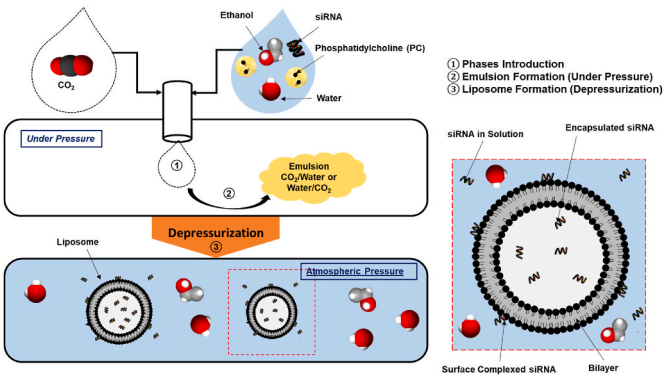

Fig. 2. Schematic representation of liposome preparation using a supercritical process.

Table 1
Operating conditions for the experimental design.

Experiment	Pressure (bar)	Temperature (°C)	Phospholipid mass ratio (wt %)
1	90	40	1
2	150	35	1
3	90	45	1
4	150	45	1
5	90	40	0.1
6	150	40	0.1
7	90	40	1.9
8	150	40	1.9
9	120	35	0.1
10	120	45	0.1
11	120	35	1.9
12	120	45	1.9
13	120	40	1

3 levels for each factor was considered. The three pressure levels considered were 90, 120 and 150 bar, the three temperature levels were 35, 40 and 45 °C and the three levels of phospholipid mass ratio in the feed solution were 0.1, 1 and 1.9 wt%. The design and the calculation were performed using AZURAD software (AZURAD SAS, Marseille, France). The temperature range studied, from 35 °C to 45 °C, was chosen in order to work under supercritical conditions. Conducting the process at the lowest temperature (35 °C) makes it possible to study the properties of liposomes at the lowest energy cost operating conditions. The high temperature (45 °C) was set to be able to work with thermosensitive molecules without the risk of degrading the molecules of interest during their encapsulation. The pressure range chosen (90–150 bar) was also chosen to be in supercritical conditions. The choice of a range of rather low pressures is in accordance with an energy optimization approach.

2.6. Phase composition in the millifluidic device

The phase composition in the millifluidic device was calculated through several steps.

The residence times of $scCO_2$ and of the feed solution were calculated considering the mass flow rates of $scCO_2$ (at the operating conditions of pressure and temperature) and of the feed solution.

The mass of $scCO_2$ flowing through the millifluidic device at working pressure was calculated by using $scCO_2$ density at the operating conditions (NIST WebBook, National Institute of Standards and Technology, Gaithersburg, Maryland, United States). Knowing the residence time of $scCO_2$ in the millifluidic device, the mass of $scCO_2$ flowing through the millifluidic device was calculated.

The mass flow rate of the feed solution was calculated, the density of the solution at 25 °C being measured. Knowing the mass fraction of water and ethanol in the solution, the mass flow rates of water and ethanol were calculated. Thanks to the residence time of the feed solution in the millifluidic device, it was possible to calculate the mass of water and ethanol flowing through the millifluidic device.

The mass fraction of water, ethanol and $scCO_2$ in the millifluidic device for each experimental condition was then calculated. The mass ratios of phospholipids in the millifluidic device, ranging from 0.05 to 1.0 wt%, were not taken into consideration because their values are much lower than the mass fractions of ethanol, water and CO_2.

2.7. Ex vivo test

2.7.1. Cell culture

Human control fibroblasts from Institut Coriell (AG07095) were cultured in a complete culture medium (DMEM low glucose (Biowest, Nuaille, France) supplemented with 15% fetal calf serum (Gibco, Loughborough, UK) and 2 mM L-Glutamine (Gibco, Loughborough, UK)) in T25 flasks (Dutscher, Bernolsheim, France) placed in an oven (humid

atmosphere, 5% CO_2 and 37 °C).

2.7.2. siRNA transfection

In order to investigate siRNA transfection, 120 000 cells were seeded with 2 mL of complete medium in wells of a 6-well plate (VWR, Radnor, PA, USA). 24 h after plating, 30 nM of siRNA specifically targeting the *LMNA* transcript (3′UTR region) or siRNA not targeting any gene (negative control) were transfected with 3 different vectors:

- JetPRIME ® which contains a cationic polymer-based molecule acting as encapsulating agent (Polyplus Transfection, Illkirch, France).
- INTERFERin ® (Polyplus Transfection, Illkirch, France).
- Liposomes prepared by supercritical millifluidic process.

2.7.3. Protein extraction

After a siRNA transfection time of 48 h, the cells were lysed, and the total proteins extracted by 50 μL of 1X extraction buffer. The 3X extraction buffer was prepared by mixing 9.4 mL Tris-HCl pH 6.8; 18.8 mL sodium dodecyl sulfate (SDS) 20%; 15 mL Glycerol; 6.8 mL distilled water and a pinch of Bromophenol Blue. The lysed cells were then collected by scraping into a 2 mL Eppendorf tube and sonicated 3 times 0.5 s ON/0.5 s OFF. The total proteins thus extracted were quantified using the Pierce™ BCA Protein Assay kit (Thermofisher scientific, Waltham, MA, USA).

2.7.4. Western blot (WB)

The Western blot (semi-quantitative molecular biology analysis method) allowed the detection of proteins of interest by means of antibodies specific to these proteins. Western blots (WB) were performed on 40 μg of total protein in the presence of a Chameleon TM Duo Prestained Protein Ladder molecular weight marker (LI-COR Biosciences, Lincoln, NE, USA) on a gel (Nupage 4–12% Bis-Tris Midi Gel (Thermofisher scientific, Waltham, MA, USA)). Prior to gel deposition, proteins were denatured by adding 5% of 2-mercaptoethanol and heating for 5 min at 95 °C. Migration was performed in a MES buffer (Life Technologies,Carlsbad, California, USA) at 200V for 1 h. The separated proteins were transferred to an Immobilon-FL membrane (PVDF filter, Chemicon/Millipore, USA). The membrane was then saturated with a fluorescent WB blocking buffer (#MB-070 (Rockland)) diluted ½ in 1X TBST (1X TBS prepared from 20x TBS (Thermo, 28358 Pierce™ 20X TBS Buffer) + 0.1% tween 20). The hybridization of primary antibodies was performed at room temperature with shaking for 1.5 h: mouse-derived monoclonal anti-lamine A/C IgG antibodies (sc-376248, Santa Cruz Biotechnology Inc., Santa Cruz, CA, USA) diluted at 1:5000 and mouse-derived monoclonal anti-GAPDH IgG antibodies (MAB374, Merck Millipore, Darmstadt, Germany) diluted at 1:40 000. After three 5-min washes with 1X TBST under agitation, the secondary antibodies were incubated at room temperature (20 °C) for 45 min under agitation: fluorochrome IRDye®800CW donkey anti-mouse IgG (926–32212, LI-COR Biosciences, Lincoln, NE, USA) diluted at 1:15 000. Fluorescence signals were detected on a Biorad ChemiDoc MP reader according to the manufacturer's recommendations. Relative quantification of the bands obtained for lamin A versus the housekeeping protein GAPDH were performed on ImageLab 6.1 (2020, Bio-Rad, Laboratories, Inc., Hercules, California, USA). All the *ex vivo* experiments were performed in triplicate.

3. Results and discussion

3.1. Repeatability test

The repeatability was studied by replicating three times the experiment conducted at 120 bar, 45 °C with phospholipid mass ratio in the feed solution of 0.1 wt%. The repeatability was evaluated considering the MD, the size distribution and the PDI factor curves of the liposomes formed. The results, reported in Table 2 and Fig. 3, show a satisfying repeatability of the process: the liposomes formed have a mean diameter of 130 nm distributed unimodally.

3.2. Operating conditions optimization of the millifluidic device

3.2.1. General findings

The MD, particle size distribution and PDI factor are given in Table 3. The liposomes formed with the continuous millifluidic process were all found to be unimodally distributed with mean diameters ranging from 124 nm to 166 nm.

3.2.2. Influence of the variation of operating conditions

For synthesis, the effects of operating condition variations are given in Fig. 4. The effect of pressure on the liposome MD is shown in Fig. 4 (a – c). In general, at a set phospholipid mass ratio and set temperature, an increase in pressure led to a decrease in the liposome MD. Nevertheless, these MD variations occur in a part of the experimental domain (temperature and phospholipids mass ratio), while in the other part of the experimental domain, the MD are not impacted by the pressure variation. For example, on Fig. 4 (a), an increase in pressure from 90 to 150 bar at a temperature of 35 °C led to a decrease in the liposome MD from 145 nm to 125 nm. Fig. 4(a–b) exhibits large areas where no variations of the liposome MD were observed, as for in the blue and yellow areas shown in Fig. 4 (a) and (b) respectively. Finally, in Fig. 4 (c) whatever the phospholipid mass ratio at a set temperature of 40 °C, an increase in pressure from 90 to 150 bar did not lead to a variation of liposome MD. These observations suggest that the pressure had a slight influence on the MD of liposomes for given operating conditions, but most of the time, the pressure had no significant effects on the liposome MD which is supported by the p-value of pressure parameter (Table 4) which is greater than 5% (22.469%). Moreover, in view of the modelling results and surface plots obtained, the pressure does not have a significant influence in comparison to the effect of phospholipid mass ratio on liposome MD.

The effect of pressure on the PDI factor is given in Fig. 4 (d – f). These figures highlight that contrarily to the liposome MD, pressure has an impact on the PDI factor. Indeed, whatever the set parameter, an increase of pressure led to a significant decrease of the PDI factor in the overall experimental domain suggesting a tighter size distribution since only unimodal distributions were obtained for all operating conditions.

To deepen these observations, the mass fractions of water, ethanol and $scCO_2$ flowing through the millifluidic device were calculated and reported in Table 5. It was found that the mass fractions of water (ranging from 43.33 to 58.37 wt%) were always the highest compared to ethanol and $scCO_2$ mass fractions. This highest amount corresponds to a two-phase system in the millifluidic device: a water-rich phase and a CO_2-rich phase. Indeed, the compositions in the millifluidic device were compared with the CO_2-ethanol-water phase diagram proposed in the work of Durling et al. [41] for a temperature of 40 °C and pressures of 100, 200 and 300 bar. For all the operating conditions of pressure and temperature tested in the experimental design, two distinct phases are present in the millifluidic device after mixing of the different compounds. Being largely in the "two-phase" zone of the diagram and not at the limit of the zone, a slight variation in temperature around 40 °C may

Table 2
Mean Diameter and PDI of liposome obtained during repeatability test.

Experiment	Mean Diameter (MD) ± SD (nm)	Size Distribution	PDI ± SD
10–1	130.6 ± 3.3	Unimodal	0.292 ± 0.001
10–2	128.9 ± 8.6	Unimodal	0.33 ± 0.06
10–3	129.9 ± 1.1	Unimodal	0.276 ± 0.006

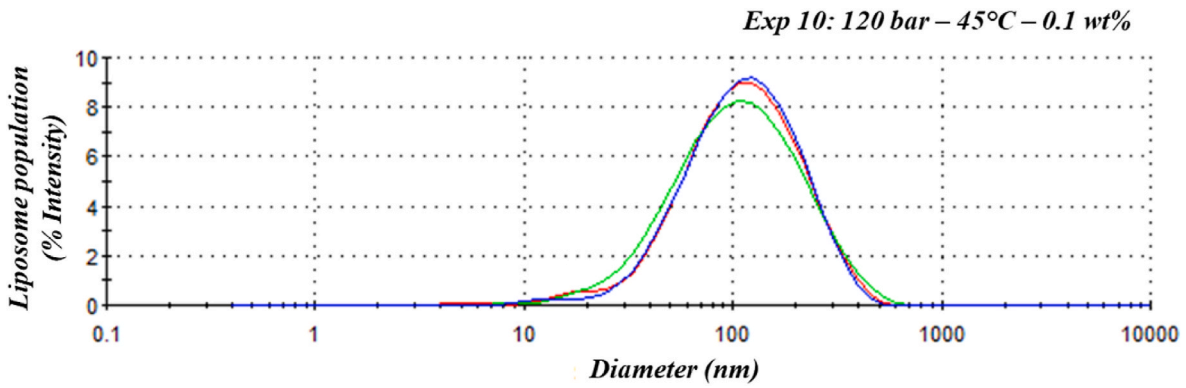

Fig. 3. Size distribution obtained in repeatability tests for continuous millifluidic process.

Table 3
MD, size distribution and PDI factor of the formed liposomes at the studied experimental conditions.

Experiment	P (bar)	T (°C)	C (wt %)	MD ± SD (nm)	Size Distribution	PDI ± SD
1	90	40	1	154.6 ± 7.0	Unimodal	0.425 ± 0.001
2	150	35	1	147.2 ± 3.6	Unimodal	0.298 ± 0.003
3	90	45	1	123.9 ± 3.0	Unimodal	0.426 ± 0.001
4	150	45	1	143.0 ± 2.4	Unimodal	0.384 ± 0.002
5	90	40	0.1	130.0 ± 1.4	Unimodal	0.269 ± 0.002
6	150	40	0.1	125.8 ± 0.8	Unimodal	0.254 ± 0.002
7	90	40	1.9	148.4 ± 0.5	Unimodal	0.37 ± 0.08
8	150	40	1.9	155.6 ± 2.2	Unimodal	0.306 ± 0.003
9	120	35	0.1	131.1 ± 1.6	Unimodal	0.28 ± 0.02
10	120	45	0.1	130.6 ± 3.3	Unimodal	0.292 ± 0.001
11	120	35	1.9	165.7 ± 1.6	Unimodal	0.37 ± 0.03
12	120	45	1.9	146.5 ± 2.3	Unimodal	0.31 ± 0.03
13	120	40	1	134.0 ± 3.9	Unimodal	0.33 ± 0.04

From experimental results for MD and PDI, the polynomial coefficients of Eq. (1) were determined by multilinear regression and are given in Table 4.

not significantly affect the number of phases in presence in the millifluidic device. The proportion of $scCO_2$ in the millifluidic device varies according to the operating conditions of pressure and temperature. The mass fraction of $scCO_2$ ranged from 25.92 wt% (45 °C and 90 bar) to 45.01 wt% (35 °C and 150 bar).

The highest fractions of $scCO_2$ flowing through the millifluidic device were found for the highest pressures. This observation can be correlated with the evolution of the PDI factor with increasing pressure: the higher the amount of $scCO_2$ in the millifluidic tube during phospholipid injection, the tighter the size distribution of the liposomes formed. Similar results were observed in the work of Zhao et al. [42]. In this present work, the correlation between pressure and size distribution is consistent since the liposomes are formed during the depressurization. Indeed, at high pressures, the depressurization takes place with a greater pressure drop compared to lower processing pressures. As a result, the expansion of the emulsion during depressurization is more brutal because the quantity of CO_2 released is greater. Therefore, the release of a higher amount of CO_2 leads to the formation of liposomes with narrower size distributions and lower PDI factors due to a faster organization of the phospholipids into liposomes with a more brutal separation of the CO_2. Indeed, a higher process pressure corresponds to a higher pressure drop, leading to enhanced mass transfers during the liposome formation. Therefore, a higher processing pressure resulted in a better uniformity of the liposomes.

The effect of temperature is given in Fig. 4 (a-b): at a set phospholipid mass ratio and pressure, an increase in temperature led to a decrease in liposome MD. This effect is more pronounced when the phospholipid mass ratio is 1 wt% (Fig. 4 (b)). At the lowest phospholipid mass ratio (Fig. 4 (a)), the variation on liposome MD with increasing temperature is negligible when the pressures are higher than 125 bar. According to Fig. 4 (a), the liposomes with the smallest MD (125 nm represented by the blue area) are formed at the lowest phospholipid mass ratio when the temperature is close to 35 °C and the pressure higher than 130 bar. And according to Fig. 4 (b), the liposomes with the smallest MD (135 nm represented by the green area) are formed at the highest phospholipid mass ratio when the temperature is close to 42 °C and the pressure higher than 120 bar. These variations suggest that the phospholipid mass ratio should also be considered with temperature variations. On Fig. 4(d–e) the variations of temperature, whatever the set operating conditions, did not lead to a significant variation of the PDI factor. As a result, temperature and phospholipid concentration have an impact on the average size of the liposomes (as seen in Table 4). However, temperature has no impact on the size distribution (PDI value) of the liposomal suspensions formed.

The influence of the variations of phospholipid mass ratio upon liposome MD is given in Fig. 4 (c). At a given pressure and temperature, increasing the phospholipid mass ratio led to an increase in the liposome MD in the overall experimental domain from 130 to 150 nm. Considering the previous observations on temperature and pressure effects and the p-value in Table 4, phospholipid mass ratio appears to have a very significant effect on the liposome MD. These observations can be explained with the nature of the phases in the Winsor system. Depending on the system studied, there may be the presence of either a single phase, two phases (CO_2-in-water emulsion or water-in-CO_2 emulsion) or three phases (water-rich, CO_2-rich and mid-phase emulsion). These Winsor systems are systems where water and CO_2 are introduced in the same quantities and where the surfactant is introduced at different concentrations. The ternary pressurized system Water/CO_2/Surfactant can have one or more phases depending on the operating conditions (temperature, pressure). The different behaviors of the phases as a function of the surfactant concentration and the operating conditions (temperature and pressure) are described in Fig. 5. Four types of behavior can be observed. According to the notations introduced by Winsor, the first observable behavior is type I (or $\underline{2}$) where the surfactant has a better affinity with CO_2. Therefore, the CO_2 in Water microemulsion is in equilibrium with a water-rich phase. This microemulsion appears as normal micelles. The second observable behavior is the type II (or $\overline{2}$)

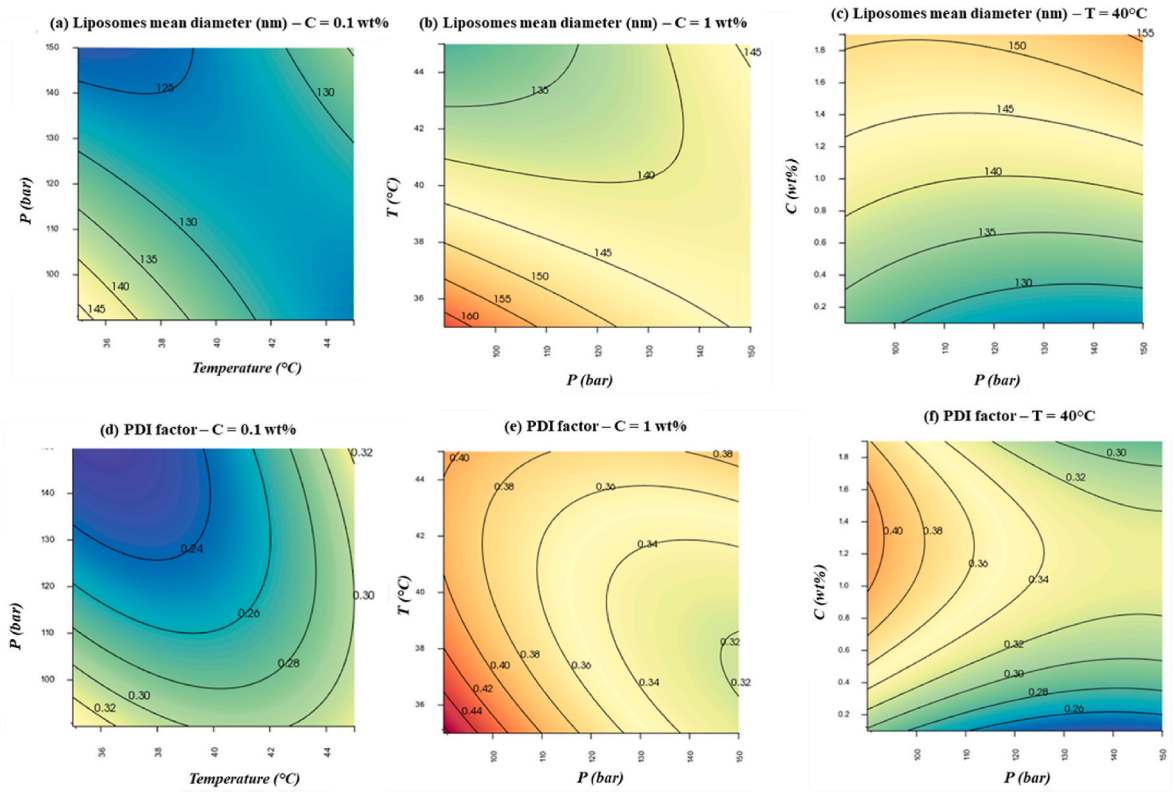

Fig. 4. Response surface plots of formed liposomes MD (a) at a set phospholipid mass ratio of 0.1 wt%, (b) at a set phospholipid mass ratio of 1 wt%, (c) at a set temperature of T = 40 °C and PDI factor (d) at a set phospholipid mass ratio of 0.1 wt%, (e) at a set phosp phospholipid mass ratio of 1 wt%, (f) at a set temperature of T = 40 °C as function of pressure, temperature and phospholipid mass ratio in the feed solution.

Table 4
Regression coefficients of the polynomial model and analysis of the variance for the effects of pressure, temperature, and phospholipid mass ratio on the MD and PDI factor of formed liposomes (*p < 0.05, **p < 0.01, and ***p < 0.001).

Coefficients	MD	Standard deviation for MD	p-Value for MD	PDI	Standard deviation for PDI	p-Value for PDI
b_0	139.928	0.792	–	0.34327	0.03148	–
b_1 (P)	−0.579	0.334	0.22469	−0.03823	0.01326	0.03447*
b_2 (T)	−7.477	0.338	0.00203**	0.00138	0.01343	0.92210
b_3 (C)	12.055	0.287	<0.00100***	0.03145	0.1141	0.03999*
$b_{1\text{-}1}$ (P-P)	2.235	0.587	0.06265	0.02096	0.02336	0.41070
$b_{2\text{-}2}$ (T-T)	3.362	0.592	0.02960*	0.03142	0.02353	0.23923
$b_{3\text{-}3}$ (C-C)	−0.732	0.528	0.29997	−0.06241	0.02099	0.03104*
$b_{1\text{-}2}$ (P-T)	8.494	0.579	0.00461**	0.03084	0.02302	0.23806
$b_{1\text{-}3}$ (P-C)	2.85	0.427	0.02174*	−0.01150	0.01699	0.52846
$b_{2\text{-}3}$ (T-C)	−5.241	0.383	0.0053**	−0.01810	0.01524	0.28824

Table 5
Phase mass fractions flowing through the millifluidic device.

Temperature (°C)	P (bar)	Water (wt%)	EtOH (wt%)	$scCO_2$ (wt%)
35	90	48.91	13.16	37.93
	120	45.04	12.12	42.84
	150	43.33	11.66	45.01
40	90	53.89	14.50	31.61
	120	46.62	12.55	40.83
	150	44.40	11.95	43.65
45	90	58.37	15.71	25.92
	120	48.52	13.06	38.42
	150	45.59	12.27	42.14

behavior and describes a system where the Water in CO_2 microemulsion in the form of reverse micelles is in equilibrium with a CO_2 rich phase. The third Winsor behavior (type III) describes a three-phase system where the microemulsion is in equilibrium between a CO_2-rich phase and a water-rich phase. Finally, the last Winsor system (type IV behavior) is characterized by the presence of a single phase containing the microemulsion.

The behaviour of the system under pressure is directly related to the concentration of the surfactant (here phospholipids). The use of higher surfactant contents leads to an increase in the diameter of the micelles formed. The work of Lesoin et al. [40], based on observations of emulsions under pressure and on granulometric analyses, shows that the higher the water/lipid mass ratio, the smaller the diameter of the liposomes formed and vice versa. For the same amount of water in the autoclave, the increase in phospholipid concentration induces an increase in the average diameter of the liposomes formed. Table 5 shows that over the whole operating range, the water compositions in the autoclave for the batch process do not vary significantly. Based on the work of Lesoin et al. [40], the increase in liposome size can be directly correlated to the increase in phospholipid content. These observations can be explained by the nature of the phases present in the autoclave as a

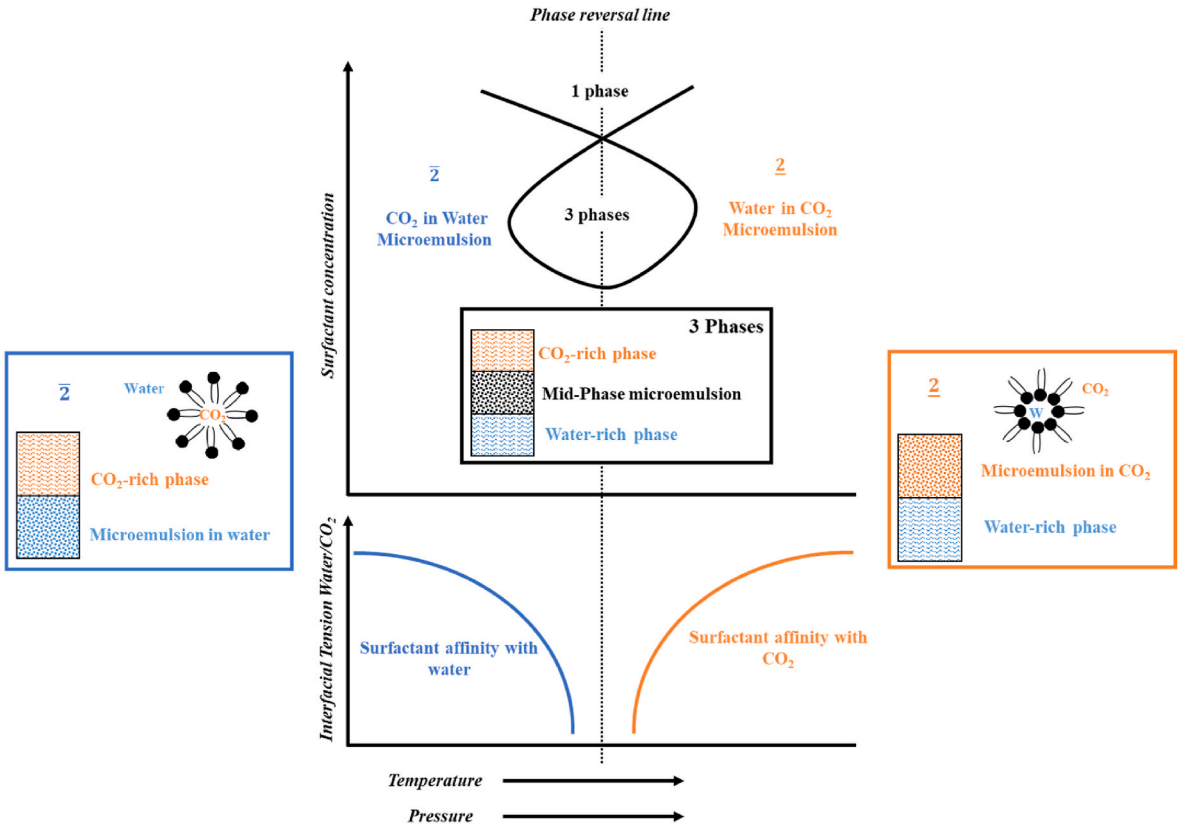

Fig. 5. Winsor systems as a function of surfactant concentration, interfacial tension and operating conditions of temperature and pressure.

function of the surfactant (phospholipid) concentration. The significant effect of the phospholipid mass ratio can also be explained by the increase in phospholipid mass ratio flowing through the millifluidic device which can lead to a change in the equilibria of the emulsions under pressure. This change has been studied by Lesoin et al. [40] who showed that the higher water/phospholipid ratio allows the preparation of liposomes with the smallest diameter. Therefore, as the mass fraction of water flowing through the millifluidic device was systematically about 50 wt%, the increase in phospholipid concentration directly induces an increase in liposome size. The increase in liposome size with the concentration of phospholipids was also observed by Reverchon et al. [43]. The higher phospholipid content promotes contact between the phospholipids, resulting in the organisation of several bilayers, forming multilamellar liposomes.

The influence of the variations of phospholipid mass ratio upon the PDI factor is shown in Fig. 4 (f). Increasing the phospholipid mass ratio up to about 1.1% at set pressures and temperatures leads to an increase in the PDI factor (from 0.28 to 0.38 at 100 bar and 40 °C). At higher mass ratio, no variations of the PDI factors were observed (about 0.38 at 100 bar and 40 °C). The lowest PDI factor (0.26) was found at the lowest phospholipid mass ratio.

Considering these overall results, the optimal operating conditions allowing the formation of liposomes with the smallest MD and the smallest size distribution (lowest PDI value) is 150 bar, 35 °C and a phospholipid mass ratio of 0.1 wt% in the feed solution. In order to confirm the predictive model of MD and PDI of liposomes, a test with these operating conditions was carried out. When using the millifluidic process at these optimized operating conditions, the liposomes obtained in the liposome's suspensions are distributed in a unimodal population with a PDI of 0.245 ± 0.003 with average diameters of 125.2 ± 2.2 nm. The results obtained are in good agreement with the defined mathematical model and confirm the validity of the model in the studied operating area.

3.3. siRNA encapsulation and transfection assay

Encapsulated siRNAs targeting *LMNA* represent an innovative therapeutic approach for the treatment of progeria. Two different siRNAs were encapsulated using the millifluidic device: a siRNA specifically targeting the *LMNA* transcript (siLMNA) and a siRNA non-targeting any gene (Control) allowing the comparison of the results of the different formulations. The experiments were carried out at the optimal operating conditions established in the previous sections: 150 bar, 35 °C and a phospholipid mass ratio in the feed solution of 0.1 wt% in the operating area studied.

Using these operating conditions, liposomes with MD ranging between 120 and 130 nm were produced (liposomes diameters were respectively 125.2 ± 2.2 nm without siRNA and 123.6 ± 4.4 nm with siARN) The mean diameter of the liposomes obtained is similar with or without siRNA encapsulation. The liposomal suspensions recovered at the end of the process had a siRNA concentration of 5 μM (for siLMNA and Control). After ethanol removal by rotavapor, the siRNA concentrations in the liposomal suspensions increased to 6.5 μM. These concentrations correspond to the amount of RNA in the feed solution. The ethanol-free liposomal suspensions were used to treat cells in culture at a final concentration of siRNAs of 30 nM, and lamin A expression in these cells was quantified by WB. The expression of the housekeeping protein GAPDH was also quantified as a loading control because it is constitutively expressed in almost all tissues in high amounts. The results are shown as lamin A/GAPDH ratio to allow the comparison of the different transfection agents (JetPrime; INTERFERin and liposomes prepared in supercritical medium). In all conditions, the effect of the *LMNA*-targeted siRNA was compared to the effect of the control.

The results, presented in Fig. 6, show the decrease in lamin A expression when using all three transfection agents. The lamin A/GAPDH ratio decreased from 0.51 to 0.23 between control and RNA assays for JetPrime, from 0.52 to 0.22 for INTERFERin and from 0.59 to

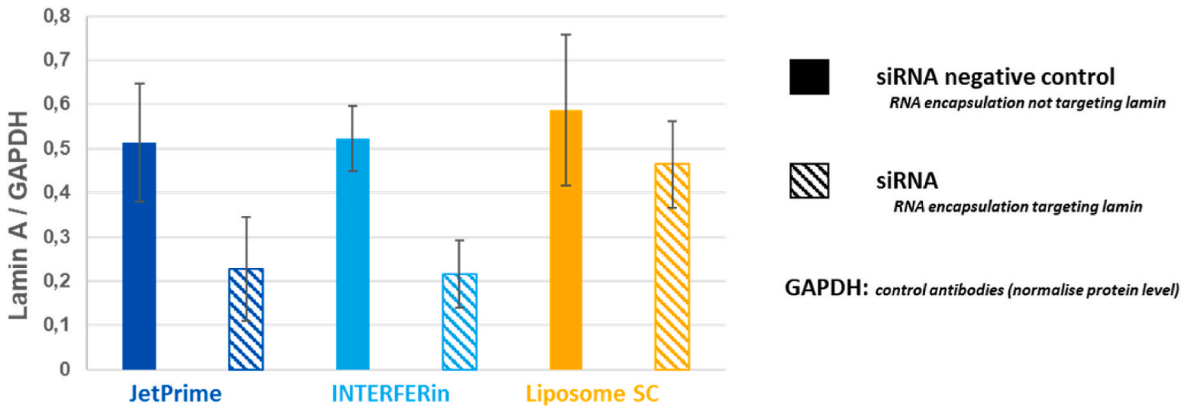

Fig. 6. Average results of Western blot quantification of lamin A for three transfection agents (JetPrime; INTERFERin and supercritical processed liposomes).

0.46 for supercritical liposomes. However, the decrease in lamin A expression was only significant for the JetPrime and INTERFERin assays. Indeed, the decrease observed for the assays when using liposomes is only a trend as it remains within the error range of the measurements. However, the use of liposomes as transfection agents appears to have a major advantage over the other two agents. Indeed, transfections performed with liposomes were much less toxic for the cells than transfections performed with commercial vectors (JetPrime and INTERFERin). The toxicity of the formulations was not quantified but simply carried out with visual observations during the transfection assays.It is important to underline that the formulations developed in this work enabled WB results coherent with the results obtained with the two other commercial vectors even if the lamin A/GAPDH ratios obtained are higher than for the two commercial vectors. These results demonstrate that the cells were not damaged by the formulations and that the liposomes formed by the supercritical millifluidic process developed during this study can be used to develop effective formulations for siRNA transfection. The advantage of this process is that it can be used to produce formulations for patients, either small batches for a clinical study, or larger commercial batches. As mentioned above, the scale-up of the process can be performed by numbering-up the millifluidic devices. This scale-up mode ensures the production of industrial batches exhibiting similar properties to the lab-scale batches. Nevertheless, before scaling up the process and implementing it, it is important to complete the study. Indeed, the preliminary tests presented in this study have demonstrated the feasibility of the process, however they must be completed and deepened to develop conditions to observe a significant decrease of the lamina during cells essays. These new tests will be particularly important to adapt the RNA concentration in the formulations.

4. Conclusion

The continuous millifluidic process allows the formation of liposomes with MD ranging between 123.9 ± 3.0 nm and 165.7 ± 1.6 nm depending on the studied experimental conditions. The optimal operating conditions for the formation of liposomes with low MD were found to be 150 bar, 35 °C with a phospholipid mass ratio of 0.1 wt% in the feed solution (in the operating area studied). The formed liposomes are distributed in a unimodal population with a PDI of 0.24 with average diameters of 125 nm. It is therefore possible to consider this process for the formation of liposomes in gene therapy (application of liposomes with diameters below 150 nm). The millifluidic process optimization studies concluded that the most influential parameter for controlling the characteristics of the liposomes formed is the phospholipid mass ratio in the feed solution. Pressure does not significantly influence the liposomes size (MD) but it has an impact on size distribution of liposomes (PDI) in liposomal suspension (higher pressure results in tighter size distribution). The millifluidic process was applied for the encapsulation of siRNAs in order to develop a potential new therapy for the treatment of progeria. The resulting formulations were compared to commercial transfection agents *ex vivo* by measuring lamin A expression by WB. These first results show that the liposomes prepared in supercritical medium containing siRNAs targeting *LMNA* allow a decrease in the expression of lamin A (major goal – decrease not yet significant for these feasibility tests). Moreover, the liposomes developed in the framework of this study are not damaging to cells in culture and seem to be safer than the commercial transfection agents generally used for this type of transfection.

Author declaration

We wish to confirm that there are no known conflicts of interest associated with this publication and there has been no significant financial support for this work that could have influenced its outcome.

We confirm that the manuscript has been read and approved by all named authors and that there are no other persons who satisfied the criteria for authorship but are not listed. We further confirm that the order of authors listed in the manuscript has been approved by all of us.

We confirm that we have given due consideration to the protection of intellectual property associated with this work and that there are no impediments to publication, including the timing of publication, with respect to intellectual property. In so doing we confirm that we have followed the regulations of our institutions concerning intellectual property.

We further confirm that any aspect of the work covered in this manuscript that has involved either

experimental animals or human patients has been conducted with the ethical approval of all relevant bodies and that such approvals are acknowledged within the manuscript.

We understand that the Corresponding Author is the sole contact for the Editorial process (including Editorial Manager and direct communications with the office). He/she is responsible for.

36729795967 16communicating with the other authors about progress, submissions of revisions and final approval of proofs. We confirm that we have provided a current, correct email address which is accessible by the Corresponding Author.

Declaration of competing interest

The authors declare that they have no known competing financial interests or personal relationships that could have appeared to influence the work reported in this paper.

Data availability

Data will be made available on request.

References

[1] C.D. Novina, P.A. Sharp, The RNAi revolution, Nature 430 (2004) 161–164, https://doi.org/10.1038/430161a.

[2] R. Wilson, J.A. Doudna, Molecular mechanisms of RNA interference, Annu. Rev. Biophys. 42 (2013) 217–239, https://doi.org/10.1146/annurev-biophys-083012-130404.

[3] M.A. Behlke, Progress towards in vivo use of siRNAs, Mol. Ther. 13 (2006) 644–670, https://doi.org/10.1016/j.ymthe.2006.01.001.

[4] N. Agrawal, P.V.N. Dasaradhi, A. Mohmmed, P. Malhotra, R.K. Bhatnagar, S. K. Mukherjee, RNA interference: biology, mechanism, and applications, Microbiol. Mol. Biol. Rev. 67 (2003) 657–685, https://doi.org/10.1128/MMBR.67.4.657-685.2003.

[5] I. Friedrich, A. Shir, S. Klein, A. Levitzki, RNA molecules as anti-cancer agents, Semin. Cancer Biol. 14 (2004) 223–230, https://doi.org/10.1016/j.semcancer.2004.04.001.

[6] S.K. Radhakrishnan, T.J. Layden, A.L. Gartel, RNA interference as a new strategy against viral hepatitis, Virology 323 (2004) 173–181, https://doi.org/10.1016/j.virol.2004.02.021.

[7] R.K.M. Leung, P.A. Whittaker, RNA interference: from gene silencing to gene-specific therapeutics, Pharmacol. Ther. 107 (2005) 222–239, https://doi.org/10.1016/j.pharmthera.2005.03.004.

[8] Y. Zeng, B.R. Cullen, RNA interference in human cells is restricted to the cytoplasm, RNA 8 (2002) 855–860.

[9] I.R. Gilmore, S.P. Fox, A.J. Hollins, M. Sohail, S. Akhtar, The design and exogenous delivery of siRNA for post-transcriptional gene silencing, J. Drug Target. 12 (2004) 315–340, https://doi.org/10.1080/10611860400006257.

[10] S. Akhtar, I.F. Benter, Nonviral delivery of synthetic siRNAs in vivo, J. Clin. Invest. 117 (2007) 3623–3632, https://doi.org/10.1172/JCI33494.

[11] M. Çağdaş, A.D. Sezer, S. Bucak, Liposomes as Potential Drug Carrier Systems for Drug Delivery, Application of Nanotechnology in Drug Delivery, 2014, https://doi.org/10.5772/58459.

[12] J. Halder, A.A. Kamat, C.N. Landen, L.Y. Han, S.K. Lutgendorf, Y.G. Lin, W. M. Merritt, N.B. Jennings, A. Chavez-Reyes, R. Coleman, D.M. Gershenson, R. Schmandt, S.W. Cole, G. Lopez-Berestein, A.K. Sood, Erratum: focal adhesion kinase targeting using in vivo short interfering RNA delivery in neutral liposomes for ovarian carcinoma therapy, Clin. Cancer Res. 12 (2019) 4916–4924, https://doi.org/10.1158/1078-0432.CCR-19-1132, 10.1158/1078-0432.CCR-06-0021) SMASH, Clinical Cancer Research. 25 (2019) 3194.

[13] D.V. Morrissey, J.A. Lockridge, L. Shaw, K. Blanchard, K. Jensen, W. Breen, K. Hartsough, L. Machemer, S. Radka, V. Jadhav, N. Vaish, S. Zinnen, C. Vargeese, K. Bowman, C.S. Shaffer, L.B. Jeffs, A. Judge, I. MacLachlan, B. Polisky, Potent and persistent in vivo anti-HBV activity of chemically modified siRNAs, Nat. Biotechnol. 23 (2005) 1002–1007, https://doi.org/10.1038/nbt1122.

[14] S. Jafari, S. Maleki Dizaj, K. Adibkia, Cell-penetrating peptides and their analogues as novel nanocarriers for drug delivery, Bioimpacts 5 (2015) 103–111, https://doi.org/10.15171/bi.2015.10.

[15] J. Gao, W. Liu, Y. Xia, W. Li, J. Sun, H. Chen, B. Li, D. Zhang, W. Qian, Y. Meng, L. Deng, H. Wang, J. Chen, Y. Guo, The promotion of siRNA delivery to breast cancer overexpressing epidermal growth factor receptor through anti-EGFR antibody conjugation by immunoliposomes, Biomaterials 32 (2011) 3459–3470, https://doi.org/10.1016/j.biomaterials.2011.01.034.

[16] J.-Y. Fang, T.-L. Hwang, Y.-L. Huang, Liposomes as vehicles for enhancing drug delivery via skin routes, Curr. Nanosci. 2 (2006) 55–70.

[17] G. Bozzuto, A. Molinari, Liposomes as nanomedical devices, Int. J. Nanomed. 10 (2015) 975–999, https://doi.org/10.2147/IJN.S68861.

[18] A. Akinc, M.A. Maier, M. Manoharan, K. Fitzgerald, M. Jayaraman, S. Barros, S. Ansell, X. Du, M.J. Hope, T.D. Madden, B.L. Mui, S.C. Semple, Y.K. Tam, M. Ciufolini, D. Witzigmann, J.A. Kulkarni, R. van der Meel, P.R. Cullis, The Onpattro story and the clinical translation of nanomedicines containing nucleic acid-based drugs, Nat. Nanotechnol. 14 (2019) 1084–1087, https://doi.org/10.1038/s41565-019-0591-y.

[19] J. Wang, J.D. Byrne, M.E. Napier, J.M. DeSimone, More effective nanomedicines through particle design, Small 7 (2011) 1919–1931, https://doi.org/10.1002/smll.201100442.

[20] A.D. Bangham, Properties and uses of lipid vesicles: an overview, Ann. N. Y. Acad. Sci. 308 (1978) 2–7, https://doi.org/10.1111/j.1749-6632.1978.tb22010.x.

[21] B. Maherani, E. Arab-Tehrany, M.R. Mozafari, C. Gaiani, M. Linder, Liposomes: a review of manufacturing techniques and targeting strategies, CNANO 7 (2011) 436–452, https://doi.org/10.2174/157341311795542453.

[22] C.I. Nkanga, A.M. Bapolisi, N.I. Okafor, R.W.M. Krause, General Perception of Liposomes: Formation, Manufacturing and Applications, Liposomes - Advances and Perspectives, 2019, https://doi.org/10.5772/intechopen.84255.

[23] Y.P. Patil, S. Jadhav, Novel methods for liposome preparation, Chem. Phys. Lipids 177 (2014) 8–18, https://doi.org/10.1016/j.chemphyslip.2013.10.011.

[24] D.D. Lasic, Applications of liposomes, in: Handbook of Biological Physics, Elsevier, 1995, pp. 491–519, https://doi.org/10.1016/S1383-8121(06)80027-8.

[25] M.H.W. Milsmann, R.A. Schwendener, H.-G. Weder, The preparation of large single bilayer liposomes by a fast and controlled dialysis, Biochim. Biophys. Acta Biomembr. 512 (1978) 147–155, https://doi.org/10.1016/0005-2736(78)90225-0.

[26] D. Lombardo, M.A. Kiselev, Methods of liposomes preparation: formation and control factors of versatile nanocarriers for biomedical and nanomedicine application, Pharmaceutics 14 (2022) 543, https://doi.org/10.3390/pharmaceutics14030543.

[27] T.P. Castor, Methods and apparatus for making liposomes, US5554382A, https://patents.google.com/patent/US5554382A/en, 1996. (Accessed 10 July 2020).

[28] L. Frederiksen, K. Anton, P. van Hoogevest, H.R. Keller, H. Leuenberger, Preparation of liposomes encapsulating water-soluble compounds using supercritical carbon dioxide, J. Pharmaceut. Sci. 86 (1997) 921–928, https://doi.org/10.1021/js960403q.

[29] L.A. Meure, N.R. Foster, F. Dehghani, Conventional and dense gas techniques for the production of liposomes: a review, AAPS PharmSciTech 9 (2008) 798, https://doi.org/10.1208/s12249-008-9097-x.

[30] I.E. Santo, R. Campardelli, E.C. Albuquerque, S.V. de Melo, G. Della Porta, E. Reverchon, Liposomes preparation using a supercritical fluid assisted continuous process, Chem. Eng. J. 249 (2014) 153–159, https://doi.org/10.1016/j.cej.2014.03.099.

[31] L. Lesoin, C. Crampon, O. Boutin, E. Badens, Preparation of liposomes using the supercritical anti-solvent (SAS) process and comparison with a conventional method, J. Supercrit. Fluids 57 (2011) 162–174, https://doi.org/10.1016/j.supflu.2011.01.006.

[32] S. Kunastitchai, L. Pichert, N. Sarisuta, B.W. Müller, Application of aerosol solvent extraction system (ASES) process for preparation of liposomes in a dry and reconstitutable form, Int. J. Pharm. 316 (2006) 93–101, https://doi.org/10.1016/j.ijpharm.2006.02.051.

[33] E. Badens, Mise en forme de principes actifs pharmaceutiques en phase supercritique, Techniques de l'ingénieur, 2012, p. 24.

[34] A.D. Sandre-Giovannoli, R. Bernard, P. Cau, C. Navarro, J. Amiel, I. Boccaccio, S. Lyonnet, C.L. Stewart, A. Munnich, M.L. Merrer, N. Lévy, Lamin A truncation in hutchinson-gilford progeria, Science (2003), https://doi.org/10.1126/science.1084125.

[35] K. Harhouri, D. Frankel, C. Bartoli, P. Roll, A. De Sandre-Giovannoli, N. Lévy, An overview of treatment strategies for Hutchinson-Gilford Progeria syndrome, Nucleus 9 (2018) 265–276, https://doi.org/10.1080/19491034.2018.1460045.

[36] N. Bonello-Palot, S. Simoncini, S. Robert, P. Bourgeois, F. Sabatier, N. Levy, F. Dignat-George, C. Badens, Prelamin A accumulation in endothelial cells induces premature senescence and functional impairment, Atherosclerosis 237 (2014) 45–52, https://doi.org/10.1016/j.atherosclerosis.2014.08.036.

[37] Y. Murakami, K. Inoue, R. Akiyama, Y. Orita, Y. Shimoyama, LipTube: liposome Formation in the tube process using supercritical CO2, Ind. Eng. Chem. Res. 61 (2022) 14598–14608, https://doi.org/10.1021/acs.iecr.2c02095.

[38] L. Lesoin, C. Crampon, O. Boutin, E. Badens, Development of a continuous dense gas process for the production of liposomes, J. Supercrit. Fluids 60 (2011) 51–62, https://doi.org/10.1016/j.supflu.2011.04.018.

[39] I. Söderberg, Phase behavior and structure in the soybean phosphatidylcholine-ethanol-water system, in: B. Lindman, J.B. Rosenholm, P. Stenius (Eds.), Surfactants and Macromolecules: Self-Assembly at Interfaces and in Bulk, Steinkopff, Darmstadt, 1990, pp. 285–289, https://doi.org/10.1007/BFb0118270.

[40] L. Lesoin, O. Boutin, C. Crampon, E. Badens, CO2/water/surfactant ternary systems and liposome formation using supercritical CO2: a review, Colloids Surf. A Physicochem. Eng. Asp. 377 (2011) 1–14, https://doi.org/10.1016/j.colsurfa.2011.01.027.

[41] N.E. Durling, O.J. Catchpole, S.J. Tallon, J.B. Grey, Measurement and modelling of the ternary phase equilibria for high pressure carbon dioxide–ethanol–water mixtures, Fluid Phase Equil. 252 (2007) 103–113, https://doi.org/10.1016/j.fluid.2006.12.014.

[42] L. Zhao, F. Temelli, Preparation of liposomes using supercritical carbon dioxide via depressurization of the supercritical phase, J. Food Eng. 158 (2015) 104–112, https://doi.org/10.1016/j.jfoodeng.2015.03.004.

[43] E. Reverchon, G. Della Porta, M.G. Falivene, Process parameters and morphology in amoxicillin micro and submicro particles generation by supercritical antisolvent precipitation, J. Supercrit. Fluids 17 (2000) 239–248, https://doi.org/10.1016/S0896-8446(00)00045-0.